

**EVALUATION OF PHYSICO-MECHANICAL,  
CHEMICAL PROPERTIES AND  
CYTOTOXICITY OF FABRICATED GLASS  
IONOMER NANO ZIRCONIA-SILICA-  
HYDROXYAPATITE HYBRID MATERIAL**

**ARBAZ SAJJAD**

**UNIVERSITI SAINS MALAYSIA**

**2020**

**EVALUATION OF PHYSICO-MECHANICAL,  
CHEMICAL PROPERTIES AND  
CYTOTOXICITY OF FABRICATED GLASS  
IONOMER NANO ZIRCONIA-SILICA-  
HYDROXYAPATITE HYBRID MATERIAL**

by

**ARBAZ SAJJAD**

**Thesis submitted in fulfilment of the requirements**

**for the degree of**

**Doctor of Philosophy**

**July 2020**

## ACKNOWLEDGEMENTS

First and foremost, let me thank Almighty GOD, creator, and protector. I cannot think of words that would begin to describe my gratitude for his bounteous blessings. I would like to express a deep sense of gratitude to my supervisor, *Assoc. Prof. Dr. Wan Zaripah Wan Bakar*, for her unquestionable guidance, support, and tolerant nature. Her relentless encouragement has led me to achieve various awards. My heartfelt gratitude to my co-supervisors, *Assoc. Prof. Dr. Dasmawati Mohamed* and *Assoc. Prof. T.P. Kannan* for their mentorship and guidance at various points in my research study. I would also thank *Prof. Ismail Ab Rahman*, for his expert advice and guidance critical to this research. I would like to express my gratitude to *Assoc. Prof. Dr. Mohd Fadhli Khamis*, Dean, School of Dental Sciences, and our past dean *Prof. Dr. Adam Husein*, for the various incentive schemes and financial supports offered. I cannot think how to thank my mother and father, for thanks seems too inadequate a word. My very existence today, is because of their love and trust and much more for which I cannot find the right words. Special appreciation is reserved for my amazing dear wife and my three kids who put up with me in my pursuit for this PhD degree and also for sticking with me through thick and thin. Special thanks to my fellow researcher and dear friend, *Dr. Imran Alam Moheet* for his timely and sound advice, scrutinizing nature and ready to help attitude. I would also like to acknowledge the support offered by *Nor Ailon Ghazali* during the early days of my research study. Finally, I would also like to express my appreciation to the Universiti Sains Malaysia for supporting this research project under Research University Grant Scheme No. RUI 1001/PPSG/812164.

## TABLE OF CONTENTS

<b>ACKNOWLEDGEMENTS .....</b>	<b>ii</b>
<b>TABLE OF CONTENTS .....</b>	<b>iii</b>
<b>LIST OF TABLES .....</b>	<b>ix</b>
<b>LIST OF FIGURES .....</b>	<b>xi</b>
<b>LIST OF EQUATIONS .....</b>	<b>xv</b>
<b>LIST OF ABBREVIATIONS .....</b>	<b>xvi</b>
<b>LIST OF SYMBOLS .....</b>	<b>xix</b>
<b>ABSTRAK .....</b>	<b>xxiv</b>
<b>ABSTRACT .....</b>	<b>xxv</b>
<b>CHAPTER ONE INTRODUCTION .....</b>	<b>1</b>
1.1 Background.....	1
1.2 Statement of Problem .....	4
1.3 Justification of Study .....	7
1.4 OBJECTIVES.....	9
1.4.1 General Objective .....	9
1.4.2 Specific Objectives .....	9
1.5 Research Question .....	10
1.6 Research Hypothesis .....	10
<b>CHAPTER TWO REVIEW OF LITERATURE.....</b>	<b>11</b>
2.1 Historical Development of Dental Restorative Materials .....	11
2.2 Evolution of Conventional GICs .....	12
2.3 Development of Resin-modified Glass Ionomer Cement .....	14
2.4 Structure of GICs.....	14

2.4.1	Macroscopic Structure .....	14
2.4.2	Mesoscopic Structure .....	15
2.4.3	Microscopic Structure .....	16
2.5	Chemical Composition of GICs .....	17
2.5.1	Composition of Ion Leachable Glasses.....	17
2.5.2	GIC Poly Acids .....	20
2.5.2 (a)	Acrylic Acid and Itaconic or Maleic Acid Copolymers.....	21
2.6	Setting Reaction of GICs.....	22
2.6.1	Ion-Leachable Phase .....	23
2.6.2	Gelation Phase .....	25
2.6.3	Maturation Phase .....	27
2.7	Classification of GICs .....	30
2.7.1	Classification I .....	30
2.7.2	Classification II.....	30
2.7.3	Classification III.....	31
2.8	Various Reinforcement Phase Incorporations in GIC Powder Composition .....	32
2.8.1	Hydroxyapatite Reinforced GICs .....	33
2.8.2	Silica reinforced GICs.....	35
2.8.3	Zirconia reinforced GICs .....	37
2.8.3 (a)	Zirconia Crystallographic Phases .....	38
2.8.3 (b)	Zirconia in Dentistry .....	41
2.9	Synthesis Techniques for Nano HA, Nano SiO <sub>2</sub> and Nano ZrO <sub>2</sub> .....	43
2.9.1	Chemical Precipitation Method .....	45
2.9.2	Sol- Gel Synthesis.....	46
2.9.2 (a)	Studies on Nano HA Sol-Gel Synthesis .....	48

2.9.2 (b) Studies on Nano SiO <sub>2</sub> Sol-Gel Synthesis .....	49
2.9.2 (c) Studies on Nano HA/SiO <sub>2</sub> Sol-Gel Synthesis .....	50
2.9.2 (d) Studies on Nano ZrO <sub>2</sub> Sol-Gel Synthesis.....	50
2.10 Characterization Instruments .....	51
2.11 Properties Critical to GICs .....	54
2.11.1 Compressive Strength .....	55
2.11.2 Flexural Strength.....	56
2.11.3 Fracture Toughness .....	58
2.11.4 Adhesion to the Tooth.....	61
2.11.5 Surface Roughness .....	64
2.11.6 Colour Stability .....	65
2.11.7 Sorption and Solubility .....	66
2.11.8 Fluoride Release.....	67
2.12 Biocompatibility .....	71
2.12.1 Cytotoxicity.....	72
2.13 Basis of Cytotoxicity Studies .....	73
2.13.1 Selection of Cell Line .....	73
2.13.1 (a) Primary Human Gingival Fibroblasts.....	73
2.13.2 Selection of Cytotoxicity Test.....	74
2.13.2 (a) <i>In Vitro</i> Tests .....	75
2.13.3 Other Considerations .....	75
2.14 MTT Assay .....	76
2.14.1 Cytotoxicity Studies on Nano Particle Reinforced Hybrid GICs .....	77
<b>CHAPTER THREE MATERIALS AND METHODS.....</b>	<b>79</b>
3.1 Introduction and Study Design .....	79

3.2	Chemicals and Research Tools.....	81
3.3	Preparation of NanoZrO <sub>2</sub> - SiO <sub>2</sub> - HA and Characterization.....	86
3.3.1	Preparation of ZrO <sub>2</sub> - SiO <sub>2</sub> - HA Nanocomposite (One-Pot Synthesis) ....	86
3.4	Characterization of Nano ZrO <sub>2</sub> - SiO <sub>2</sub> - HA Powder.....	91
3.4.1	Transmission Electron Microscopy .....	91
3.4.2	Scanning Electron Microscopy .....	91
3.4.3	Fourier Transform Infrared Spectroscopy.....	92
3.4.4	Energy Dispersive X-Ray .....	92
3.4.5	X-ray Diffraction.....	93
3.5	Preparation of GIC nano ZrO <sub>2</sub> -SiO <sub>2</sub> -HA Hybrid and Evaluation of Physico- Mechanical, Chemical Properties and Cytotoxicity .....	95
3.6	Sample Size Calculation.....	97
3.6.1	Compressive Strength .....	97
3.6.2	Flexural Strength.....	98
3.6.3	Fracture Toughness .....	98
3.6.4	Surface Roughness .....	99
3.6.5	Colour Stability .....	99
3.6.6	Sorption-Solubility.....	100
3.6.7	Fluoride Ion Release .....	100
3.6.8	Cytotoxicity.....	101
3.7	Physico-Mechanical and Chemical Properties Analysis .....	102
3.7.1	Compressive Strength Testing .....	102
3.7.2	Flexural Strength Testing.....	105
3.7.3	Fracture Toughness Testing .....	107
3.7.4	Surface Roughness Testing.....	110

3.7.5	Colour Stability Testing .....	113
3.7.6	Sorption-Solubility Testing.....	116
3.7.7	Fluoride Release Testing.....	118
3.8	Evaluation of Cytotoxicity using MTT Assay.....	120
3.8.1	Human Gingival Fibroblasts .....	120
3.8.2	Work Area and Equipment .....	121
3.8.3	Preparation of Complete Growth Medium.....	121
3.8.4	Thawing and Culturing of The Frozen Cells .....	121
3.8.5	Passaging Cells / Subculture .....	122
3.8.6	Preparation of the Test Materials and Extracts .....	124
3.8.7	Evaluation of Cytotoxicity .....	126
3.8.8	Determination of Cell Viability .....	128
3.9	Statistical Analysis .....	128
<b>CHAPTER FOUR RESULTS AND DISCUSSION .....</b>		<b>130</b>
4.1	Characterization of Nano Powders .....	130
4.1.1	SEM Evaluation of NanoZrO <sub>2</sub> -SiO <sub>2</sub> -HA Powder.....	130
4.1.2	TEM Evaluation of NanoZrO <sub>2</sub> -SiO <sub>2</sub> -HA Powder.....	132
4.1.3	EDX Analysis and Dot Mapping of NanoZrO <sub>2</sub> -SiO <sub>2</sub> -HA Powder.....	135
4.1.4	FTIR Evaluation of NanoZrO <sub>2</sub> -SiO <sub>2</sub> -HA Powder .....	137
4.1.5	XRD of NanoZrO <sub>2</sub> -SiO <sub>2</sub> -HA Powder .....	139
4.2	Characterization of GIC 5% NanoZrO <sub>2</sub> -SiO <sub>2</sub> -HA Composite .....	142
4.2.1	EDX Analysis and Dot Mapping of GIC nanoZrO <sub>2</sub> -SiO <sub>2</sub> -HA Hybrid..	142
4.2.2	FTIR Spectra of GIC 5% nanoZrO <sub>2</sub> -SiO <sub>2</sub> -HA Hybrid .....	144
4.3	Physico-Mechanical Properties of GIC nanoZrO <sub>2</sub> -SiO <sub>2</sub> -HA .....	146
4.3.1	Compressive Strength Evaluation.....	147



4.3.2 Flexural Strength Evaluation .....	152
4.3.3 Fracture Toughness Evaluation.....	158
4.3.4 Surface Roughness Evaluation .....	165
4.3.5 Colour Stability Evaluation.....	170
4.3.6 Sorption-Solubility Evaluation .....	178
4.4 Chemical Property Evaluation of GIC nanoZrO <sub>2</sub> -SiO <sub>2</sub> -HA.....	181
4.4.1 Fluoride Ion Release Evaluation.....	181
4.5 Cytotoxicity Evaluation of GIC 5% nanoZrO <sub>2</sub> -SiO <sub>2</sub> -HA .....	186
4.5.1 MTT Assay .....	193
<b>CHAPTER 5 CONCLUSIONS AND RECOMENDATIONS .....</b>	<b>199</b>
5.1 Conclusions .....	199
5.2 Limitations and Future work .....	200
5.3 Clinical Significance .....	201
<b>REFERENCES.....</b>	<b>203</b>
<b>APPENDICES</b>	
<b>APPENDIX A: ETHICAL APPROVAL</b>	
<b>APPENDIX B: LIST OF PUBLICATIONS</b>	
<b>APPENDIX C: LIST OF CONFERENCES &amp; AWARDS</b>	
<b>APPENDIX D: LIST OF POSTERS PRESENTED</b>	
<b>APPENDIX E: PATENT APPLICATION</b>	
<b>APPENDIX F: PLAGIARISM REPORT</b>	

## LIST OF TABLES

	Page
Table 2.1: Powder composition of the earliest GIC .....	18
Table 2.2: Minimum values of certain physico-mechanical properties needed for dental water based cements adapted from Sidhu and Nicholson(2016) ..	54
Table 3.1: The composition of GIC Fuji IX (GC Corporation, Japan) .....	81
Table 3.2: List of chemicals and materials .....	82
Table 3.3: List of tools and equipment .....	83
Table 3.4: Powder composition of nano ZrO <sub>2</sub> - SiO <sub>2</sub> - HA composite .....	88
Table 3.5: Raw quantities of the chemicals and reagents used in one-pot synthesis of nanoZrO <sub>2</sub> -SiO <sub>2</sub> -HA composite .....	88
Table 3.6: Specifications of the XRD machine.....	93
Table 3.7: Control and experimental testing groups .....	96
Table 3.8: Experimental group details and respective sample size for physico- mechanical testing.....	101
Table 4.1: The mean compressive strength of cGIC and GIC nanoZrO <sub>2</sub> -SiO <sub>2</sub> -HA using one-way ANOVA.....	147
Table 4.2: The mean flexural strength of cGIC and GIC nanoZrO <sub>2</sub> -SiO <sub>2</sub> -HA using one-way ANOVA.....	152
Table 4.3: The mean fracture toughness of cGIC and GIC nanoZrO <sub>2</sub> -SiO <sub>2</sub> -HA using one-way ANOVA.....	158
Table 4.4: The mean surface roughness of cGIC and GIC nanoZrO <sub>2</sub> -SiO <sub>2</sub> -HA using one-way ANOVA.....	165
Table 4.5: Mean L*a*b* values at the various time intervals .....	170

Table 4.6: Colour change ( $\Delta E$ ) between the various time intervals using repeated measures ANOVA .....	172
Table 4.7: Colour change ( $\Delta E$ ) between day one (baseline) and the other time intervals using repeated measures ANOVA .....	173
Table 4.8: Mean sol-sorption for experimental groups using Independent t-test ....	178
Table 4.9: Evaluation of fluoride release (ppm) from cGIC and GIC 5% nano ZrO <sub>2</sub> -SiO <sub>2</sub> -HA over 28 days .....	181
Table 4.10: Mann Whitney test results for 24 h incubation period .....	187
Table 4.11: Mann Whitney test results for 72 h incubation period .....	188

## LIST OF FIGURES

	Page
Figure 2.1: Graphical representation of the macroscopic structure of the GIC matrix at the GIC-tooth interface. ....	15
Figure 2.2: Molecular structure of the polysalt bridge proposed by Wilson(1974)...	16
Figure 2.3: Illustration of the chemical structure of GIC polyacids .....	21
Figure 2.4: Schematic illustration of what is thought to occur during the setting .....	24
Figure 2.5: Trivalent Al ion attached to three COOH groups and form $\text{Al}(\text{H}_2\text{O})_6^{3+}$ in the presence of water .....	27
Figure 2.6: Graphical representation of the cascade of events that take place at the atomic level during the setting reaction of GIC .....	29
Figure 2.7: The three polymorphic phases of zirconia (a) monoclinic,(b) tetragonal,(c) cubic (Hannink <i>et al.</i> , 2000).....	40
Figure 2.8: Schematic illustration of the sol-gel manufacturing process for nano HA. Adapted from Sadat-Shojai <i>et al.</i> (2013).....	47
Figure 2.9: Compressive stress ( $S_C$ ), shear stress( $S_S$ ) and tensile stress ( $S_T$ ) resolution in a cylindrical sample when load is applied.....	55
Figure 2.10: Schematic illustration of a 3-point bend test where L represents the span length, b and h represent the sample width and height respectively .....	57
Figure 2.11: Mode-I tensile fracture on a sample with a pre-crack for straight line fracture growth upon load application .....	59
Figure 2.12: Schematic illustration of a SEVNB sample being cracked using a 3-point bend test where L is the span length, a is the crack height, b and h represent the sample width and height respectively .....	60

Figure 2.13: Schematic illustration of the ion- exchange interfacial zone between GIC and tooth/ hydroxyapatite.....	62
Figure 2.14: SEM scan of interfacial ion- exchange layer formation between GIC and tooth substrate (Adapted from Ngo <i>et al.</i> , 1997).....	63
Figure 3.1: Flowchart summary of this study .....	80
Figure 3.2: Flow chart of the preparation of GIC nanoZrO <sub>2</sub> - SiO <sub>2</sub> - HA hybrid .....	89
Figure 3.3: Schematic illustration of preparation of Nano ZrO <sub>2</sub> - SiO <sub>2</sub> - HA, (a) CaOH dissolved in H <sub>2</sub> O,(b) H <sub>3</sub> PO <sub>4</sub> added and suspension stirred for 48 h,(c) ZrO <sub>2</sub> and TEOS added and suspension stirred for additional 12 h .....	90
Figure 3.4: Various analytical instruments used for characterization of nano powder .....	94
Figure 3.5: The powder of nanoZrO <sub>2</sub> -SiO <sub>2</sub> -HA and cGIC was mixed using a mortar and pestle in a controlled grinding technique .....	96
Figure 3.6: Flow chart of the preparation of GIC Nano ZrO <sub>2</sub> -SiO <sub>2</sub> -HA hybrid .....	97
Figure 3.7: Sample preparation for compressive strength testing.....	103
Figure 3.8: Compressive strength testing.....	104
Figure 3.9: Schematic illustration of compressive strength test .....	104
Figure 3.10: Flexural strength sample fabrication and testing.....	106
Figure 3.11: Schematic illustration of flexural strength test.....	106
Figure 3.12: SEVNB sample preparation for fracture toughness .....	108
Figure 3.13: Single-edge V notch samples subjected to fracture toughness testing using universal testing machine .....	109
Figure 3.14: Disc shaped sample fabrication for surface roughness with numbering on the underside.....	111

Figure 3.15: Surface roughness measurement using a profilometer .....	112
Figure 3.16: Colour stability measurement.....	115
Figure 3.17: Sample preparation for sorption and solubility .....	116
Figure 3.18: Samples stored in artificial saliva prior to being weighed a second time (m2).....	118
Figure 3.19: Steps involved in fluoride ion measurement .....	120
Figure 3.20: Thawing, retrieval and culturing of HGF for cytotoxicity testing.....	122
Figure 3.21: Photomicrograph of HGF at confluence in a T-25 culture flask .....	124
Figure 3.22: Preparation of material extract (a) samples removed from mould,(b) UV sterilization of samples and (c) samples immersed in complete growth medium .....	125
Figure 3.23: Two sets of 96 well culture plates prepared for each group.....	127
Figure 4.1: SEM micrographs of nanoZrO <sub>2</sub> -SiO <sub>2</sub> -HA powder (a) low magnification (100000×), (b) low magnifications(70000×) and (c) high magnification (200000×).....	131
Figure 4.2: TEM images of nanoZrO <sub>2</sub> -SiO <sub>2</sub> -HA at (a) lower magnification (100,000×) and (b) higher magnification (200,000×) .....	134
Figure 4.3: Energy dispersive x-ray spectrum showing the main elements present in the nanoZrO <sub>2</sub> -SiO <sub>2</sub> -HA powder .....	136
Figure 4.4: SEM dot mapping characteristics for (a) Zr, (b) Ca, (c) P and (d) Si in the nanoZrO <sub>2</sub> -SiO <sub>2</sub> -HA powder .....	136
Figure 4.5: FTIR spectra of nanoZrO <sub>2</sub> -SiO <sub>2</sub> -HA powder .....	138
Figure 4.6: XRD of nanoZrO <sub>2</sub> -SiO <sub>2</sub> -HA powder .....	141
Figure 4.7: Energy dispersive x-ray spectrum showing that the main elements present in the GIC nanoZrO <sub>2</sub> -SiO <sub>2</sub> -HA .....	143

Figure 4.8: SEM dot mapping characteristics for (a) Al, (b) Si, (c) Ca, (d) F, (e) P and (f) Zr in the GIC nanoZrO <sub>2</sub> -SiO <sub>2</sub> -HA.....	143
Figure 4.9: FTIR spectra of GIC 5% nanoZrO <sub>2</sub> -SiO <sub>2</sub> -HA hybrid .....	145
Figure 4.10: FTIR spectra of cGIC (Fuji IX) (Adapted from Gatin <i>et al.</i> , 2008)....	146
Figure 4.11: Compressive strength evaluation of cGIC and GIC nanoZrO <sub>2</sub> -SiO <sub>2</sub> -HA .....	149
Figure 4.12: Flexural strength evaluation of GIC nanoZrO <sub>2</sub> -SiO <sub>2</sub> -HA .....	154
Figure 4.13: Fracture toughness evaluation of GIC nanoZrO <sub>2</sub> -SiO <sub>2</sub> -HA .....	160
Figure 4.14: Surface roughness evaluation of GIC nanoZrO <sub>2</sub> -SiO <sub>2</sub> -HA .....	167
Figure 4.15: Colour change evaluation between various time intervals for GIC nanoZrO <sub>2</sub> -SiO <sub>2</sub> -HA .....	174
Figure 4.16: Colour change evaluation between baseline and other time intervals for GIC nanoZrO <sub>2</sub> -SiO <sub>2</sub> -HA .....	175
Figure 4.17: Graphical representation of sorption-solubility between GIC 5% nanoZrO <sub>2</sub> - SiO <sub>2</sub> - HA and cGIC .....	179
Figure 4.18: Fluoride ion release evaluation of GIC nanoZrO <sub>2</sub> -SiO <sub>2</sub> -HA over a 28 day period.....	183
Figure 4.19: Cell viability percentage of HGFs after 24 h incubation with GIC nanoZrO <sub>2</sub> -SiO <sub>2</sub> -HA and cGIC .....	190
Figure 4.20: Cell viability percentage of HGFs after 72 h incubation with GIC nanoZrO <sub>2</sub> -SiO <sub>2</sub> -HA and cGIC .....	191

## LIST OF EQUATIONS

	Page
Glass + H <sup>+</sup> → Ca <sup>2+</sup> + Al <sup>3+</sup> + SiO <sub>4</sub> <sup>4-</sup> (2.1) .....	23
<i>n</i> SiO <sub>4</sub> <sup>4-</sup> + 4 <i>n</i> H <sup>+</sup> → (SiO <sub>2</sub> ) × 2 <i>n</i> H <sub>2</sub> O (2.2) .....	23
Ca <sup>2+</sup> + 2PA <sup>-</sup> → Ca(PA) <sub>2</sub> (2.3) .....	26
Al <sup>3+</sup> + 2PA <sup>-</sup> → Al(PA) <sub>2</sub> <sup>+</sup> (2.4) .....	26
Ca(PA) <sub>2</sub> + Al <sup>3+</sup> → Al(PA) <sub>2</sub> <sup>+</sup> + Ca <sup>2+</sup> (2.5) .....	28
Al <sup>3+</sup> + PO <sub>4</sub> <sup>3-</sup> → AlPO <sub>4</sub> (2.6) .....	29
M(OR) <sub>4</sub> + H <sub>2</sub> O → M(OH) <sub>4</sub> + 4ROH (2.7) .....	47
M(OH) <sub>4</sub> + M(OH) <sub>4</sub> → (OH) <sub>3</sub> M-O-M (OH) <sub>3</sub> + H <sub>2</sub> O (2.8) .....	47
[F]c = ([F]1x √t)/(t + t 1/2) + √t (2.9) .....	69
CS = 4P/πd <sup>2</sup> (3.1) .....	103
FS = 3FL/2bh <sup>2</sup> (3.2) .....	105
K <sub>Q</sub> = (P <sub>Q</sub> S)/(BW <sup>3/2</sup> ) × F(a/W) (3.3) .....	108
F(a/W) = 3(a/W) <sup>1/2</sup> × 1.99 - (a/W) (1 - a/W) (1 - a/W) (3.4) .....	108
ΔE = [(ΔL*) <sup>2</sup> + (Δa*) <sup>2</sup> + (Δb*) <sup>2</sup> ] <sup>1/2</sup> (3.5) .....	114
NBS = ΔE × 0.92 (3.6) .....	115
W <sub>sp</sub> = m <sub>2</sub> - m <sub>3</sub> / V (3.7) .....	117
W <sub>sl</sub> = m <sub>1</sub> - m <sub>3</sub> / V (3.8) .....	117
% of viability = sample mean / sample -ve control × 100 (3.9) .....	128
Particle size = 0.94*λ/β Cos θ (4.1) .....	140
Particle size = 0.94 × 0.1548 <sup>-9</sup> / 0.4 Cos (16°)* = 21.62 nm (4.2) .....	140



## LIST OF ABBREVIATIONS

ADA	American dental association
AIC	Apatite ionomer cement
ANOVA	Analysis of variance
ANSI	American national standard institute
ASPA	Alumino silicate polyacrylic acid
ASTM	American Society of testing and materials
BAG	Bio-active glass
BO	Bridging oxygen
Ca/P	Calcium/phosphorus
cGIC	Conventional glass ionomer cement
CIE	Commission internationale de l'éclairage
Corp	Corporation
CP/MAS NMR	Cross polarization/magic angle spinning nuclear magnetic resonance
CR	Composite resin
CS	Compressive strength
CTE	Co-efficient of thermal expansion
DMSO	Dimethylsulphoxide
EDX	Energy dispersive x-ray
FBS	Foetal bovine serum
FS	Flexural strength
FTIR	Fourier transform infra-red
GIC	Glass ionomer cement

GPC	Glass polyalkenoate cement
HA	Hydroxyapatite
HA/ZrO <sub>2</sub>	Hydroxyapatite/zirconia
HEMA	2-hydroxyethyl methacrylate
HGF	Human gingival fibroblasts
ICDD	International centre for diffraction data
ICP	Inductively coupled plasma
IEL	Ion-exchange layer
IR	Infrared
ISE	Ion specific electrode
ISO	International organization for standards
KBr	Potassium bromide
MEM- $\alpha$	Alpha minimal essential medium
MTT	3-(4,5-dimethylthiazol-2-yl)-2,5-diphenyl tetrazolium bromide
nano-Ag	Nano-silver
Nano-FA	Nano-fluorapatite
nano-HA	Nano-hydroxyapatite
nano-HA-SiO <sub>2</sub>	Nano-hydroxyapatite-silica
nano-HA-SiO <sub>2</sub> -GIC	Nano-hydroxyapatite-silica-glass ionomer cement
nano-Zr-SiO <sub>2</sub> -HA	Nano-zirconia-silica-hydroxyapatite
nano-ZrO <sub>2</sub>	Nano-zirconia
NBO	Non bridging oxygen
NBS	National Bureau of Standards
NMR	Nuclear magnetic resonance

PAA	Poly acrylic acid
PBS	Phosphate buffered saline
pH	Potential hydrogen
PS	Particle size
PVC	Polyvinyl chloride
PMMA	Polymethyl methacrylate
RMGIC	Resin modified glass ionomer cement
rpm	Rounds per minutes
SBF	Simulated body fluid
SBS	Shear bond strength
SD	Standard deviation
SEM	Scanning electron microscope
SEM/EDX	Scanning electron microscope/Energy dispersive x-ray
SEVN/SEVNB	Single Edge V-Notched beam
sol	Solution
SR	Surface roughness
SSF	Spherical silica fillers
TEM	Transmission electron microscope
T <sub>g</sub>	Glass transition temperature
TISAB	Total ionic strength adjustment buffer
WHO	World health organization
XRD	X-ray diffraction
ZOE	Zinc oxide eugenol

## LIST OF SYMBOLS

$\sim$	Approximately
$\text{Ag}^+$	Silver ion
$\text{Ag}_2\text{O}$	Silver oxide
$\text{Al}$	Aluminium
$\text{Al}_2\text{O}_3$	Almina
$\text{Al}_2\text{O}_3\text{-SiO}_2\text{-CaF}_2$	Fluoro-alumino-silicate
$\text{Al}^{3+}$	Aluminium ion
$\text{AlF}_3$	Aluminium fluoride
$\text{AlF}_3$	Aluminium trifluoride
$\text{AlPO}_4$	Aluminium phosphate
ART	Atraumatic restorative technique
b	Breadth
Ba	Barium
$\text{Ba}^{2+}$	Barium cation
$\text{BaSO}_4$	Barium sulphate
Ca	Calcium
$\text{Ca(OH)}_2$	Calcium hydroxide
$\text{Ca}_{10}(\text{PO}_4)_6(\text{OH})_2$	Hydroxyapatite crystal
$\text{Ca}^{2+}$	Calcium ion
$\text{Ca}_3(\text{PO}_4)_2$	Calcium phosphate
$\text{CaF}_2$	Calcium fluoride
$\text{CaO}$	Calcium oxide
$\text{CO}_2$	Carbon dioxide

COO-	Carboxylate
COOH	Carboxylic acid
d	Thickness
d	Diameter
EtOh	Ehtnol
F	Fluoride
F	Force
F <sup>-</sup>	Fluoride ion
G	Gram
NH <sub>2</sub>	Amides
NH <sub>3</sub>	Ammonia
Na <sub>3</sub> AlF <sub>6</sub>	Cryolite
°C	Degree centigrade
Mg <sub>2</sub> SiO <sub>4</sub>	Forsterite
K <sub>C</sub>	Fracture stress
MPa• m <sup>1/2</sup>	Fracture toughness unit
HF <sub>2</sub>	Hydrogen fluoride
HEMA	Hydroxylethyl methacrylate
K	Kelvin
Kg	Kilogram
La	Lanthium
L	Length
Mg	Magnesium
m	Mass
Mpa	Mega pascal

mN	Meganewton
M(OR) <sub>n</sub>	Metal alkoxides
ms	Milisecond
hkl	Millers indices
Nano-SiO <sub>2</sub>	Nano-silica
nm	Nanometer
Nb <sub>2</sub> O <sub>5</sub>	Niobium pentoxide
H <sub>3</sub> PO <sub>4</sub>	Phosphoric acid
K <sub>IC</sub>	Plane–strain fracture toughness
KBr	Potassium bromide
n	Sample size
H <sub>4</sub> SiO <sub>4</sub>	Silicic acid
NaF	Sodium fluoride
Na <sup>+</sup>	Sodium ion
Na <sub>2</sub> O	Sodium oxide
H <sub>2</sub> O	Water
OH <sup>-</sup>	Hydroxide
P	Phosphorus
P/L	Powder liquid ratio
Ra	Surface roughness value
Si	Silicate
Si(OH) <sub>4</sub> •X(H <sub>2</sub> O)	Silicious hydro gel
Si <sup>4+</sup>	Silica ion
SiO <sub>2</sub>	Silica
SiO <sub>2</sub> -Al <sub>2</sub> O <sub>3</sub> -CaF <sub>2</sub>	Calcium fluoroaluminosilicate

$\text{SiO}_2\text{-Al}_2\text{O}_3\text{-CaO}$	Calcium aluminosilicate
$\text{SiO}_4$	Silicate
Sr	Strontium
$\text{Sr}^{2+}$	Strontium ion
SrO	Strontium oxide
$\beta$	Beta (power of the study)
$t_{1/2}$	Half life
TEOS	Tetraethylorthosilicate
$\text{TiO}_2$	Titanium dioxide
V	Volume
$W_{\text{sl}}$	Water solubility
$W_{\text{sp}}$	Water sorption
Wt	Weight
wt %	Weight percentage
$\text{YbF}_3$	Ytterbium fluoride
Zn	Zinc
$\text{Zn}_5(\text{OH})_8\text{Cl}_2 \cdot \text{H}_2\text{O}$	Zinc oxychloride
ZnO	Zinc oxide
$\text{ZrO}_2$	Zirconia
$\alpha$	Level of significance
$\delta$	Difference in Population Means
$\Delta E$	Color change
$\mu\text{m}$	Micrometer

**PENILAIAN KE ATAS CIRI-CIRI FIZIKO-MEKANIKAL, KIMIA DAN  
SITOTOKSISITI FABRIKASI BAHAN HIBRID NANO ZIRKONIA-SILIKA  
HIDROKSIAPATIT IONOMER KACA**

**ABSTRAK**

Tujuan kajian ini adalah untuk mensintesis dan mencirikan komposit nano zirkonia-silika-hidroksiapatit ( $\text{nanoZrO}_2\text{-SiO}_2\text{-HA}$ ) dan untuk menyiasat kesan penambahan  $\text{nanoZrO}_2\text{-SiO}_2\text{-HA}$  kepada simen ionomer kaca konvensional (cGIC).  $\text{NanoZrO}_2\text{-SiO}_2\text{-HA}$  telah disintesis menggunakan teknik sol-gel satu-pot, yang kemudiannya dicirikan menggunakan mikroskop pengimbasan elektron (SEM), mikroskop transmisi elektron (TEM), spektroskopi fourier transformasi inframerah (FTIR) dan x-ray difraksi (XRD). Berikutan kajian pencirian, siasatan lanjut telah dilakukan selepas penambahan  $\text{nanoZrO}_2\text{-SiO}_2\text{-HA}$  kepada cGIC (GIC  $\text{nanoZrO}_2\text{-SiO}_2\text{-HA}$ ) pada peratusan yang berbeza (~3% hingga 9%) untuk membandingkan sifat-sifat mekanikal mereka (kekuatan mampatan, kekuatan lenturan, dan ketahanan patah), ciri-ciri fizikal (kekasaran permukaan, kestabilan warna dan kelarutan-penyerapan), ciri-ciri kimia (pelepasan ion fluorida) dan sitotoksisiti berhubung dengan cGIC (Fuji IX). Imej SEM dan TEM telah berjaya menunjukkan bahawa morfologi partikel dari segi saiz ke pengedaran bentuk adalah kecil dan sempit dengan aglomerasi yang rendah. Serbuk nano terdiri daripada kristal HA berbentuk rod (~114 nm) yang diselaraskan dengan partikel bulat silika (~18 nm) dan zirkonia (~39 nm). Spektrum FTIR menunjukkan wujudnya beberapa interaksi molekul antara  $\text{nanoZrO}_2\text{-SiO}_2\text{-HA}$  dan GIC. Diffractogram XRD menunjukkan kehadiran puncak untuk  $\text{ZrO}_2$ ,  $\text{SiO}_2$  dan HA. Kekuatan mampatan, kekuatan lenturan dan ketahanan patah GIC 5%  $\text{nanoZrO}_2\text{-SiO}_2\text{-HA}$  secara statistik lebih tinggi daripada peratusan GIC  $\text{nanoZrO}_2\text{-SiO}_2\text{-HA}$  yang lain dan cGIC. Nilai tertinggi yang telah direkodkan ialah kekuatan



mampatan ( $144.12 \pm 13.88$  MPa), kekuatan lenturan ( $18.12 \pm 2.33$  MPa) dan ketahanan patah ( $1.35 \pm 0.15$  MPa.m<sup>1/2</sup>), membawa kepada peningkatan sebanyak ~30%, ~ 26% dan ~ 57%, berbanding dengan cGIC. Selain itu, GIC 5% nanoZrO<sub>2</sub>-SiO<sub>2</sub>-HA mempunyai profil kekasaran ( $0.158\mu\text{m} \pm 0.29$ ) sama dengan cGIC ( $0.151\mu\text{m} \pm 0.29$ ). Secara keseluruhannya, nilai perubahan warna ( $\Delta E$ ) bagi kumpulan GIC 5% nanoZrO<sub>2</sub>-SiO<sub>2</sub>-HA adalah lebih rendah berbanding dengan cGIC dalam tempoh 28 hari dan antara sedikit hingga ketara. GIC 5% nanoZrO<sub>2</sub>-SiO<sub>2</sub>-HA menunjukkan perbezaan yang sangat signifikan dalam melepaskan fluorida secara purata dalam semua selang masa berbanding dengan cGIC ( $p \leq 0.05$ ). Di samping itu, GIC 5% nanoZrO<sub>2</sub>-SiO<sub>2</sub>-HA merekodkan nilai penyerapan yang lebih rendah ( $23.64 \pm 2.3$   $\mu\text{gmm}^{-3}$ ) berbanding cGIC ( $36.28 \pm 2.6$   $\mu\text{gmm}^{-3}$ ) dan keterlarutan yang lebih tinggi ( $66.46 \pm 2.4$   $\mu\text{gmm}^{-3}$ ) berbanding cGIC ( $56.76 \pm 1.6$   $\mu\text{gmm}^{-3}$ ). Keputusan ujian sitotoksiti menunjukkan bahawa GIC 5% nanoZrO<sub>2</sub>-SiO<sub>2</sub>-HA mempunyai tahap sitotoksiti pada tempoh 24 jam inkubasi untuk kepekatan 200 mg/ml. Walau bagaimanapun, pada tempoh inkubasi selama 72 jam menunjukkan tindak balas sitotoksik yang lebih rendah berbanding dengan cGIC yang secara statistiknya signifikan ( $p < 0.05$ ) pada kepekatan 200 mg/ml ekstrak bahan. Penambahan nanoZrO<sub>2</sub>-SiO<sub>2</sub>-HA kepada cGIC meningkatkan dengan signifikan ciri-ciri fiziko-mekanikal, kimia dan menunjukkan tindak balas sitotoksik yang menggalakkan. Berdasarkan penemuan dari kajian baru kami ini, GIC nanoZrO<sub>2</sub>-SiO<sub>2</sub>-HA mempunyai potensi untuk dicadangkan sebagai bahan pergigian restoratif dengan pelbagai aplikasi bermula daripada restorasi kaviti, pembinaan teras dan sebagai bahan penyimenan simen.

**EVALUATION OF PHYSICO-MECHANICAL, CHEMICAL PROPERTIES  
AND CYTOTOXICITY OF FABRICATED GLASS IONOMER NANO  
ZIRCONIA-SILICA-HYDROXYAPATITE HYBRID MATERIAL**

**ABSTRACT**

The aim of this study was to synthesize and characterize a nano zirconia-silica-hydroxyapatite (nanoZrO<sub>2</sub>-SiO<sub>2</sub>-HA) composite and to investigate the effects of adding nanoZrO<sub>2</sub>-SiO<sub>2</sub>-HA to a conventional glass ionomer cement (cGIC). NanoZrO<sub>2</sub>-SiO<sub>2</sub>-HA composite was synthesized using a one-pot sol-gel technique, which was then characterized using scanning electron microscope (SEM), transmission electron microscope (TEM), fourier transform infrared spectroscopy (FTIR) and x-ray diffraction (XRD). Following the characterization studies, further investigations were carried out after addition of nanoZrO<sub>2</sub>-SiO<sub>2</sub>-HA to cGIC (GIC nanoZrO<sub>2</sub>-SiO<sub>2</sub>-HA) at varying weight percentage (~3% to 9%) to compare their mechanical properties (compressive strength, flexural strength, and fracture toughness), physical properties (surface roughness, colour stability and sorption-solubility), chemical property (fluoride ion release) and cytotoxicity in relation to cGIC (Fuji IX). SEM and TEM images were successful in demonstrating that the particle morphology in terms of size to shape distribution was small and narrow with low agglomeration. The nano powder consisted of rod-shaped HA crystallites (~114 nm) interspersed with spherical silica (~18 nm) and zirconia (~39 nm) particles. The FTIR spectra indicated some molecular interaction presented between the nanoZrO<sub>2</sub>-SiO<sub>2</sub>-HA and GIC. The XRD diffractogram indicated the presence of peaks for ZrO<sub>2</sub>, SiO<sub>2</sub> and HA. Compressive strength, flexural strength and fracture toughness of GIC 5% nanoZrO<sub>2</sub>-SiO<sub>2</sub>-HA was statistically higher than that of other percentages of GIC nanoZrO<sub>2</sub>-SiO<sub>2</sub>-HA and cGIC. The highest values recorded were- compressive

strength ( $144.12 \pm 13.88$  MPa), flexural strength ( $18.12 \pm 2.33$  MPa) and fracture toughness ( $1.35 \pm 0.15$  MPa.m<sup>1/2</sup>), leading to an increase of ~30 %, ~26 % and ~57 % respectively, as compared to cGIC. Additionally, GIC 5% nanoZrO<sub>2</sub>-SiO<sub>2</sub>-HA had a roughness profile ( $0.158\mu\text{m} \pm 0.29$ ) similar to cGIC ( $0.151\mu\text{m} \pm 0.29$ ). Overall, the color change ( $\Delta E$ ) values for GIC 5% nanoZrO<sub>2</sub>-SiO<sub>2</sub>-HA group were lower than those of cGIC over a 28 day period and were between slight to perceptible. The GIC 5% nanoZrO<sub>2</sub>-SiO<sub>2</sub>-HA showed highly significant difference in the mean fluoride release for all the time intervals as compared to cGIC ( $p \leq 0.05$ ). In addition, GIC 5% nanoZrO<sub>2</sub>-SiO<sub>2</sub>-HA recorded lower sorption values ( $23.64 \pm 2.3$   $\mu\text{gmm}^{-3}$ ) as compared to cGIC ( $36.28 \pm 2.6$   $\mu\text{gmm}^{-3}$ ) and higher solubility ( $66.46 \pm 2.4$   $\mu\text{gmm}^{-3}$ ) as compared to cGIC ( $56.76 \pm 1.6$   $\mu\text{gmm}^{-3}$ ). The results of cytotoxicity testing showed that GIC 5% nanoZrO<sub>2</sub>-SiO<sub>2</sub>-HA demonstrated cytotoxicity at 24 h incubation for 200 mg/ml conc. However, at 72 h incubation it exhibited lower cytotoxic response as compared to cGIC which was statistically significant ( $p < 0.05$ ) at 200 mg/ml concentration of the material extract. The addition of nanoZrO<sub>2</sub>-SiO<sub>2</sub>-HA to cGIC significantly enhanced its physico-mechanical, chemical properties and demonstrated a favourable cytotoxic response. Based on the results of our recently concluded study, GIC nanoZrO<sub>2</sub>-SiO<sub>2</sub>-HA has the potential to be suggested as a restorative dental material with diverse applications ranging from cavity restoration, core build-up and as a luting material.

# CHAPTER ONE

## INTRODUCTION

### 1.1 Background

Throughout the millennia the roots of dentistry can be found as deep as the 3000 B.C. Today's clinicians are fortunate enough to have the option to choose from a plethora of biomimetic dental materials. In the middle of the 19th century amalgam was one of the first restorative dental materials used by dental practitioners (Singh *et al.*, 2017). But amalgam was a non-tooth coloured, far from perfect crude restorative material which resulted in several problems such as post placement expansion, tooth and gingival discoloration and mercury poisoning. The use of amalgam as a restorative material has since declined (Widstrom *et al.*, 1992). The second half of the 19<sup>th</sup> century saw efforts devoted to progress from using early dental materials as merely luting/lining agents to developing them for more aesthetic and restorative applications (Singh *et al.*, 2017). Subsequently many dental materials which were white in colour began to make way into the dental industry.

There is now a trend towards the use of tooth-coloured restorative materials such as glass ionomer cement (GIC) and composite resins. The International Organization for Standardization (ISO) has adopted the term glass polyalkenoate cement (GPC) which is another name for glass ionomer cement GIC (ISO-9917–1:2007). Glass Ionomer cements were first introduced to dentistry in late 1960's and have proven to be useful in various areas of dental science, such as restorative dentistry (Wilson and Kent, 1971). Glass-ionomer cements contain ion leachable fluoro-

alumino-silicate glass that can react with water soluble acids such as polyacrylic acid (PAA) to yield cement. The cement is the product of an acid-base reaction between the silicate glass as the basic component and the poly acrylic acid homo and copolymers as the acidic component (Widstrom *et al.*, 1992).

Glass ionomers is a system which is polyelectrolytic and aqueous at the same time, are easy to manipulate, bond to tooth at an ionic level, exhibit fluoride ion release and recharge, a low coefficient of thermal expansion (CTE) and decent aesthetics (Naasan and Watson, 1998). They are also biocompatible with pulp, gingival and bone tissues. However, in the clinical environment their use has become limited owing to inferior mechanical properties such low flexural strength and fracture toughness (Mount, 2002; Oliva *et al.*, 1996; Six *et al.*, 2000; Wilson and Kent, 1972). In addition, a relatively high opacity, moisture susceptibility during early setting phase and rough surface makes these materials less desirable (Croll and Nicholson, 2002; Gladys *et al.*, 1997; Wilson and Kent, 1971; Wilson and McLean, 1988). Therefore, GICs have become restricted to restoring low stress bearing areas such proximal and axial wall defects (Albers, 2002).

In order to improve the physico-mechanical properties of GIC pure silver (Ag) and gold (Au) particles were added to the glass powder. The resulting Cermet ionomer cements had higher flexural strength compared to cGIC but were still not strong enough to replace amalgam (Al-Badri and Kamel, 1994; McLean and Gasser, 1985). Later the first light cured resin-modified glass ionomer cement (RMGIC) were developed by Antonucci *et al.*, (1988) but disadvantages such as setting shrinkage and limited depth of curing were seen (Mitra, 1991b).

Other additions to the glass powder such as, metallic oxides, strontium and barium did not have a significant effect on the mechanical properties of GICs since they lacked the ability to increase the cross-linking within the glass matrix (Deb and Nicholson, 1999; Hurrell-Gillingham *et al.*, 2005). Recent research has proven that incorporation of nanoceramics such as hydroxyapatite (HA), silica (SiO<sub>2</sub>), zirconia (ZrO<sub>2</sub>) produced via various soft chemistry processes capable of creating nanoscale particles have a potential to improve the properties of GICs (Ahmad Shiekh *et al.*, 2014; Moshaverinia *et al.*, 2008a).

It is thus, imperative to assess the efficacy of various nano fillers incorporated GIC in terms of overcoming the various shortcomings of cGIC mentioned earlier. The mechanical properties such as compressive strength, flexural strength, fracture toughness can be tested using a mechanical testing machine following the international standards organization (ISO) guidelines. Similarly, physical properties like colour change, surface roughness and solubility-sorption are evaluated using a spectrophotometer, profilometer and desiccators respectively (Carvalho *et al.*, 2012; Prabhakar *et al.*, 2013; Zankuli *et al.*, 2014). Another unique property of cGIC is the ability to release F<sup>-</sup> which is evaluated using an ion specific electrode and pH meter (Arita *et al.* 2011; Panigrahi *et al.*, 2016; Sayyedani *et al.*, 2013). It is also important to make sure that any new hybrid GIC developed has a cytotoxic profile similar to cGIC if not better, which can be evaluated via a colourimetric *in vitro* assay (Ahmed *et al.* 2011; Noorani *et al.*, 2017).

## 1.2 Statement of Problem

Currently commercially available conventional GICs are brittle water-based materials with poor mechanical properties, low wear resistance, and opacity which set by an acid-base reaction. Therefore, to overcome the limitations of cGIC, RMGIC was developed. Resin modified GIC demonstrated some improved strength, but they set by a photo initiator and not by an acid-base reaction. In addition, they were found to be more cytotoxic than conventional GIC (cGIC) and demonstrated increased microleakage due to water sorption (Kent *et al.*, 1971; Smith, 1998; Wilson, 1991). Subsequently the properties of GIC's were enhanced by the addition of either metal particle, such as Au or Ag, but their inclusion brought damage to materials in relation to F<sup>-</sup> release, adhesion to tooth structure, as well as poor aesthetics (McLean *et al.*, 1985).

The incorporation of micron range sized particles, such as, alumina, zirconia or glass fibres into cGIC are some efforts made to improve the mechanical strength of cGIC (Gu *et al.*, 2005c; Kerby and Bleiholder, 1991; Lohbauer *et al.*, 2004). However, the improvement on mechanical properties was not significant. Most likely the reason for this could be the micron-size of the fillers used.

Due to the aforementioned weaknesses of cGIC, many attempts were made to improve them by incorporation of a nano reinforcement phase of HA and SiO<sub>2</sub> in cGIC. Improvements in their compressive strength, diametral tensile strength, flexural strength, fracture toughness, bonding and F<sup>-</sup> release properties have been reported but at the expense of increased microleakage and water solubility (Arita *et al.*, 2003;

Felemban and Ebrahim, 2016; Lucas *et al.*, 2003; Moshaverinia *et al.*, 2008b; Rahman *et al.*, 2017).

Furthermore, few more studies have been reported that the incorporation of a HA-SiO<sub>2</sub> phase in a cGIC resulted in enhanced mechanical properties and a favourable cytotoxic response (Ahmad Shiekh *et al.*, 2014; Noorani *et al.*, 2017; Norhayati, 2015). The authors believed that the nano SiO<sub>2</sub> particles filled the voids between the elongated HA particles, enhancing the packing density, thereby, improving the mechanical properties (Ahmad Shiekh *et al.*, 2014).

Lopes *et al.* (2018) experimented on HA added GIC and reported an increase in the surface roughness (Ra) value ( $0.20 \pm 0.07 \mu\text{m}$ ) of the tested material. An increase in surface roughness could lead to an increase in microbial adhesion, plaque accumulation and thus could lead to increased risk of caries and periodontal disease (Bollen *et al.*, 1997).

In a recent study, Rahman *et al.* (2017), evaluated the effect of the addition nanoZrO<sub>2</sub>-SiO<sub>2</sub>-HA on the hardness of cGIC. They concluded that incorporation nanoZrO<sub>2</sub>-SiO<sub>2</sub>-HA into the GIC resulted in a 54% improvement in hardness over that for cGIC. However, their study was mainly focussed with the synthesis of the nanopowder. Nonetheless, there is no detailed work available on the addition of a nanoZrO<sub>2</sub>-SiO<sub>2</sub>-HA to GIC with regards to its mechanical properties such as, compressive, flexural and fracture toughness. In addition, physical, chemical and biological properties of GIC nanoZrO<sub>2</sub>-SiO<sub>2</sub>-HA composite with regards to colour



stability, surface roughness, sorption-solubility, fluoride release and cytotoxicity are yet to be reported.

It has been suggested that different methods of synthesising nano-powder might produce a material with different characteristics. In this case, some researchers have reported different characteristics for nanoparticles (nanoZrO<sub>2</sub>, nanoSiO<sub>2</sub> and nano-HA) produced with different synthesis techniques (Rahman *et al.*, 2014; Rahman and Padavettan, 2012; Moshaverinia *et al.*, 2008a). It has been noticed that there is a lack of data on the effect of one pot sol-gel synthesis technique on the morphology and chemical composition of nanoZrO<sub>2</sub>-SiO<sub>2</sub>-HA composite.

### 1.3 Justification of Study

Nowadays, GIC is one of the most widely used restorative materials that is being employed by dentist worldwide both in urban and rural setup due to its ease of handling, cost, and beneficial anti-caries property (Tyas, 2018). It is particularly utilized in Atraumatic Restorative Treatment (ART) for high caries risk patients due to its acid-base setting mechanism and fluoride release property (Yip *et al.*, 2001a). Historically, cGICs are brittle, exhibit poor wear resistance and thus are not ideally suited for restoring posterior stress-bearing areas inside the oral cavity (Prakki *et al.*, 2005; Yip *et al.*, 2001a). Many *in-vitro* studies have compared the performance of cGICs to high-density GICs and filler modified GIC (Hussin *et al.*, 2018; Lucas *et al.*, 2003; Moshaverinia *et al.*, 2008a; Nishimura *et al.*, 2014; Panahandeh *et al.*, 2018; Prakki *et al.*, 2005; Yip *et al.*, 2001a). They found out that it still lacks the performance required as a universal restorative material.

In order to promote the usage of cGIC especially for restoration of adult teeth and for anterior teeth restorations, the physical, mechanical, and aesthetic properties must improve. Studies found that incorporation of HA-ZrO<sub>2</sub> improved the mechanical properties and F<sup>-</sup> release of GIC (Gu *et al.*, 2005b; Rajabzadeh *et al.*, 2014). Nanozirconia which is translucent may also improve the aesthetic property of GIC as shown in a study by Rahman *et al.* (2017). Many studies have been conducted to assess the physical, mechanical and biological properties of these nano fillers. A thorough review of literature has revealed that, studies documenting on the effect of addition of nanoZrO<sub>2</sub>-SiO<sub>2</sub>-HA composite to GIC on mechanical properties such as compressive, flexural strength and fracture toughness are yet to be undertaken. In addition, physical

and chemical properties of GIC nanoZrO<sub>2</sub>-SiO<sub>2</sub>-HA composite with regards to colour stability, surface roughness, sorption-solubility, fluoride release, and cytotoxicity are yet to be determined. Since there is a dearth of information on the effect of a nanoZrO<sub>2</sub>-SiO<sub>2</sub>-HA filler on the physico-mechanical properties of cGIC this study was undertaken.

The basic concept behind the current study was to synthesize nanoZrO<sub>2</sub>-SiO<sub>2</sub>-HA composite to be incorporated as a reinforcement filler into the cGIC. This incorporation of nanoZrO<sub>2</sub>-SiO<sub>2</sub>-HA into cGIC might alter the properties of GIC, thus making it a superior restorative material physico-mechanically. In addition, incorporation of nanoZrO<sub>2</sub>-SiO<sub>2</sub>-HA into cGIC can enhance the diffusion of fluoride ions at the enamel/dentine interfaces enhancing its anti-caries activity.

Therefore, the novel findings of the current study will have the potential to expand the future application of GIC in clinical practice both in urban and rural setup, thus paving the way for a wider application of GIC in restorative dentistry.

## **1.4 OBJECTIVES**

### **1.4.1 General Objective**

1. To synthesize and evaluate the physico-mechanical, chemical properties and cytotoxicity of the glass ionomer cement (GIC) nano Zirconia ( $\text{ZrO}_2$ ) -Silica ( $\text{SiO}_2$ )- Hydroxyapatite (HA) hybrid material.

### **1.4.2 Specific Objectives**

1. To synthesize the nano $\text{ZrO}_2$ -  $\text{SiO}_2$ - HA using the one-pot synthesis method for addition to cGIC and to characterize the nano $\text{ZrO}_2$ -  $\text{SiO}_2$ - HA powder synthesized from one-pot synthesis method using transmission electron microscopy (TEM), scanning electron microscopy (SEM), fourier transform infrared spectroscopy (FTIR) and x-ray diffraction (XRD).
2. To evaluate and compare the mechano-physical properties- compressive strength (CS), flexural strength (FS), fracture toughness (FT) and surface roughness (SR) of four different groups of GIC nano $\text{ZrO}_2$ - $\text{SiO}_2$ -HA respectively, with the conventional GIC.
3. To evaluate the physical properties- colour stability (over a 28-day period) and sorption-solubility of the new hybrid material group with the best mechanical properties tested and compare it with the conventional GIC.
4. To assess fluoride release from the new hybrid material group with the best mechanical properties tested over a 28-day period and compare it with the conventional GIC.

5. To compare cytotoxicity of the new hybrid material group with the best mechanical properties tested at 24 h and 72 h incubation period and compare it with the conventional GIC.

### **1.5 Research Question**

Does the incorporation of a novel nanoZrO<sub>2</sub>- SiO<sub>2</sub>- HA composite formulation in the cGIC have a significant impact on the physico-mechanical, chemical properties and cytotoxicity of cGIC?

### **1.6 Research Hypothesis**

1. The addition of nanoZrO<sub>2</sub>- SiO<sub>2</sub>- HA to the cGIC significantly increases the physical, mechanical, and chemical properties.
2. The addition of nanoZrO<sub>2</sub>- SiO<sub>2</sub>- HA to the cGIC does not exhibit any cytotoxic effect on human gingival fibroblast cell line.

## **CHAPTER TWO**

### **REVIEW OF LITERATURE**

#### **2.1 Historical Development of Dental Restorative Materials**

We live in a society, where the general population is overly concerned about their aesthetics and appearance. Therefore, it is only logical to assume that the most preferred dental restorative material should be one which closely resembles and performs as the part of the tooth it replaces throughout the life of the individual. During the 19th century silver amalgam was the most popular restorative dental materials being used by dentists all over Europe. Taveau, in France (1816), developed, the first crude dental amalgam by mixing mercury with silver coins. Needless to say, this resulted in several problems such as post placement expansion, amalgam tattoo and mercury poisoning (Anusavice, 2003).

In the 1890's the amalgam composition was fine-tuned and experimented with, till it could be successfully employed as a dental filling material. However, in spite of its advantages, such as being inexpensive, durable and easy of handling, amalgam also possessed two serious shortcomings; namely, mercury poisoning (which can cause neurodegenerative disease, and rarely birth defects, upon long term exposure), and poor aesthetics due to dark metallic colour. In the near future the use of amalgam is going to decline, in parts due to environmental restrictions and the aesthetic concerns. The development of more durable and technique insensitive restorative materials is the way to move in the correct direction (Anusavice, 2003).

## 2.2 Evolution of Conventional GICs

In the first half of the 19th century dental cements progressed from being merely used for luting and lining to being utilized as aesthetic filling materials. Subsequently various tooth-coloured dental restoratives were developed. It was Sorel (1855), who created the first dental restorative cement, zinc oxychloride ( $\text{Zn}_5(\text{OH})_8\text{Cl}_2 \cdot \text{H}_2\text{O}$ ). Later, Pierce (1879) modified and replaced  $\text{Zn}_5(\text{OH})_8\text{Cl}_2 \cdot \text{H}_2\text{O}$  with an improved zinc oxide-phosphate cements (Albers, 2002). These zinc oxyphosphates exhibited greater durability and lower pulpal irritation. Thereafter, around the turn of the 1900's, Ames and Fleck introduced modern zinc phosphates luting cements (Khurshid *et al.*, 2019). Whereas, a bit earlier in 1875, through the works of Pierce and Flagg, the zinc oxide eugenol (ZOE) cement was made available, which soon saw a rise in its demand owing to its anodyne effect (Albers, 2002).

The turn of the 19<sup>th</sup> century saw these cements being used for temporary restorations, cavity bases and as adhesives. On the other hand, silicate cement, a glass ceramic restorative material, developed by Fletcher in 1873, did not gain popularity until 1904 when Steenbock modified and reintroduced it. A few years later, Shoenbeck developed the first successful silicate cements with the addition of  $\text{F}^-$  (Khurshid *et al.*, 2019).

The Laboratory of the Government Chemists, London tried to further enhance the handling and mechanical properties of silicates, zinc polycarboxylates and zinc phosphate cements. The goal was to combine the beneficial features of the silicate cements (translucency and  $\text{F}^-$  ion release) with those of zinc polycarboxylates (chemical bond to the tooth substrate and low pulp toxicity) (Walls, 1986; Wilson and

Kent, 1971). At the aforementioned laboratory, Wilson and Kent sought to make these materials a practical system by figuring out ways to overcome their sluggish setting and hydrolytically instability.

The evolution of the GICs dates back to the early 1970s. The researchers at laboratory of government chemists were seeking to replace the silicate restorative materials. The first breakthrough came when it was suggested to replace phosphoric acid with polyacrylic acid in GIC (Smith, 1968). In doing so, the authors discovered the chemical reaction of GICs was actually the result of a neutral phenomenon between the basic component and an acidic polymer, resulting in a polysalt matrix. The cause for poor handling characteristics was identified as poor sensitivity of the basic glass to the weak polyacid. Therefore, to enhance the glass reactivity, its basic oxide ratio was increased; thereby, making the glass component more susceptible to the acidic polymer attack (Culbertson, 2001; Nagaraja Upadhya and Kishore, 2005).

In 1972 Wilson and Kent manufactured the first workable cGIC and named it aluminosilicate polyacrylate-I (ASPA-I). Unfortunately, the cement took 20 minutes to harden, and exhibited poor aesthetics because of its high  $F^-$  content which increased its opacity, thereby, limiting its clinical usability (Wilson and Kent, 1972). However, in 1972 Wilson and McLean reformulated the cement by adding tartaric acid (TA) and by replacing  $Al_2O_3$  with  $SiO_2$  in the glass (McLean and Wilson, 1977).

In 1985 McLean and Gasser with the intention to improve the properties of cGIC which set by acid-base reaction, successfully produced a glass and silver (Ag) cermet which was later commercially marketed by ESPE as Ketac-Silver® (McLean



*et al.*, 1985). They used pure Ag particles, fused to abrasion resistant calcium ASPA glass powder with a lower coefficient of friction. Unfortunately, with the passage of time silver particles in the material formed  $\text{Ag}_2\text{O}$  that resulted in discolouration of the restoration. Cermet ionomer cements had higher flexural strength compared to cGIC but were still not strong enough to replace amalgam (Al-Badri and Kamel, 1994).

### **2.3 Development of Resin-modified Glass Ionomer Cement**

In 1988 Antonucci *et al.* introduced the first light cured RMGIC with hopes to emulate the best properties of composites and GICs such as, anticariogenicity due to  $\text{F}^-$  release, low CTE and hydrophilicity of GICs. This was done by mixing cGIC with small quantity of resin polymeric solution (Wilson, 1990). The first commercial RMGIC, Vitrebond, was developed (Mitra, 1991a) set by dual mechanisms, namely a light polymerisation reaction and an acid-base reaction. Later in 1991 a self-polymerising RMGIC was introduced though, disadvantages like setting shrinkage and limited depth of curing remained (Mitra, 1991a).

### **2.4 Structure of GICs**

#### **2.4.1 Macroscopic Structure**

Glass ionomers are complex materials with a predominantly Si gel-like matrix as a result of the reaction between an aqueous PAA solution and a fluoro-alumino-silicate glass powder ( $\text{Al}_2\text{O}_3$ -  $\text{SiO}_2$ - $\text{CaF}_2$ ). The partially dissolved remnant glass cores act as fillers within in the matrix. The matrix is composed of precipitated polyacrylate salt bridges and uncoiled polymer chains (Figure 2.1).

### 2.4.2 Mesoscopic Structure

A mesoscopic structure lies between microscopic and macroscopic structures. At the mesoscopic level, GICs consist of partially consumed glass cores encapsulated in a  $\text{SiO}_4$  gel, embedded in a matrix of cross-linked  $\text{Al}^{3+}$  and  $\text{Ca}^{2+}$  polysalt bridges. Silica gel and  $\text{AlPO}_4$  make up the bulk of the matrix.

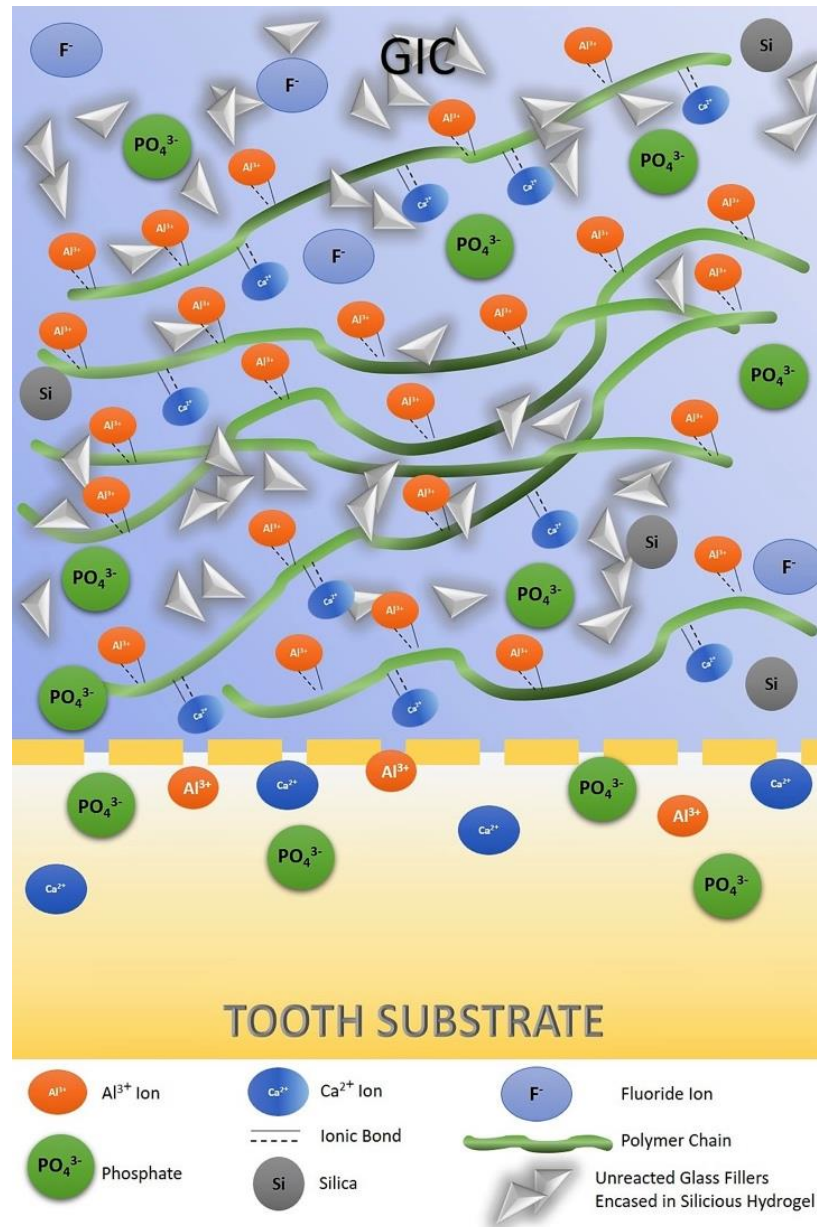


**Figure 2.1:** Graphical representation of the macroscopic structure of the GIC matrix at the GIC-tooth interface.

### 2.4.3 Microscopic Structure

At the microscopic or atomic scale, polysalt bridges are formed between the polymer chains and the  $\text{Al}^{3+}$  and  $\text{Ca}^{2+}$  cations following their chelation by tartaric acid. The glass matrix is composed of polysalt bridges formed by  $\text{Al}^{3+}$  cations cross-linking with the  $-\text{COOH}$  groups from the PAA polymer chains, in the presence of  $\text{H}_2\text{O}$  and  $\text{F}^-$  facilitating the cation binding. Fluoride is usually present in the form of complex such as  $\text{AlF}_2$ ,  $\text{AlF}_2$  and  $\text{CaF}$  (Wilson, 1978). Phosphorus usually form  $\text{AlPO}_4$  late in the setting reaction and is evenly distributed throughout the matrix (Wasson and Nicholson, 1993; Wilson, 1996a).

Wilson first proposed the possible molecular structures of the salt bridges in 1974 (Figure 2.2). Unfortunately, there has been no follow-up study nor any molecular modelling of the proposed salt bridge structures.

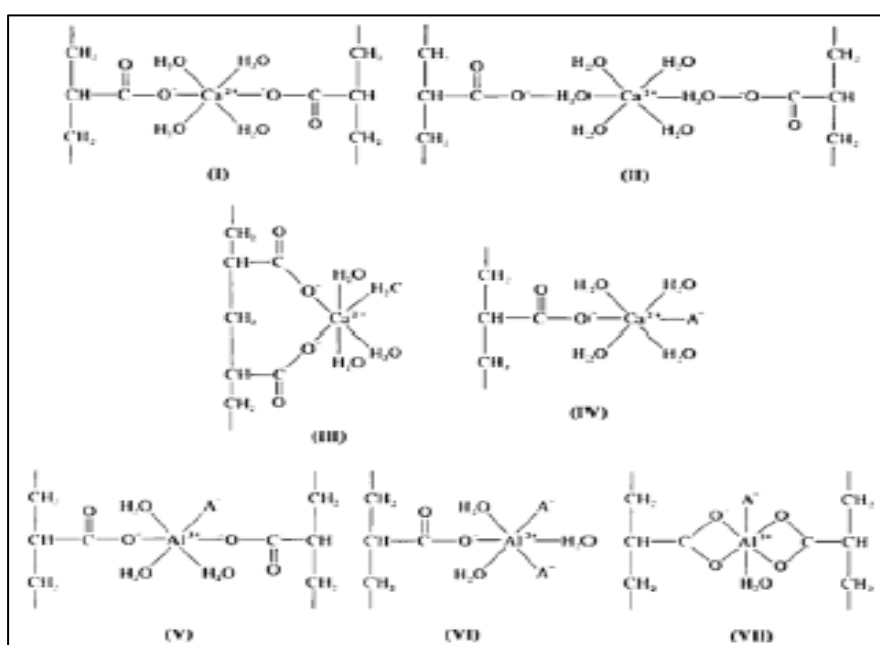


**Figure 2.2:** Molecular structure of the polysalt bridges proposed by Wilson (1974)

## **2.5 Chemical Composition of GICs**

The International Organization for Standardization (ISO) has adopted the term glass polyalkenoate cement (GPC) which is usually known as glass ionomer cement (GIC).

### **2.5.1 Composition of Ion Leachable Glasses**

The glasses used in GIC are classed as  $\text{Al}_2\text{O}_3$ -  $\text{SiO}_2$ - $\text{CaF}_2$  glasses. These are different from conventional industrial glasses which are mostly composed of soda and lime silica glasses. Routinely, the ion leachable fluoro-alumino-silicate glasses are manufactured by the melt quench or fusion method involving several inorganic chemicals, such as quartz ( $\text{SiO}_2$ ), alumina ( $\text{Al}_2\text{O}_3$ ), cryolite ( $\text{Na}_3\text{AlF}_6$ ), fluorite ( $\text{CaF}_2$ ), aluminium trifluoride ( $\text{AlF}_3$ ) as listed in Table 2.1(Clifford *et al.*, 2001).

During this process, the melt glass is shock cooled with the intention of forming coarse granules or frit which is then ground to a pulp via ball milling to create the desired particle size. Generally, a particle size of  $<20\mu\text{m}$  is produced for the luting applications and a particle size of  $<50\mu\text{m}$  is preferred for restorative or filling purposes. In both these instances, after ball milling the glass powder is acid washed with a weak poly acetic acid to render it less reactive (Wilson and McLean, 1988).

**Table 2.1:** Powder composition of the earliest GIC

Components	Percentage	Effects
SiO <sub>2</sub>	29.0	Essential component-fuse to form calcium fluoro-alumino silicate glasses.
Al <sub>2</sub> O <sub>3</sub>	16.6	
CaF <sub>2</sub>	34.2	
Na <sub>3</sub> AlF <sub>6</sub>	5.0	Reduces fusion temperature and complements CaF <sub>2</sub>
AlPO <sub>4</sub>	9.9	Adds body to cement and improves translucency
Sr,Ba,La	----	Replace Ca partially or fully to impart radiopacity to GIC

Adapted from Clifford *et al.*, (2001).

This is because of the fact that these glasses possess a highly crosslinked O-Si-O structure and are relatively stable chemically and are immune to the conventional acid attack. Therefore, it is logical to assume that such glasses would serve no purpose since in order to produce set cement it is imperative that the glass is susceptible to the poly acids and release metal cations in the process. However, by certain cations we can ensure that the O-Si-O linkage is disrupted to produce non-bridging oxygens (NBO).

These cations are classed into different groups of network constituents depending on their nature. Zachariasen proposed a classification whereby they were divided into three groups (Zachariasen, 1932):

1. Network formers ( $\text{Si}^{4+}$ ,  $\text{PO}_4^{3-}$ ),
2. Network modifiers ( $\text{Ca}^{2+}$ ,  $\text{Sr}^{2+}$ ,  $\text{Ba}^{2+}$ ,  $\text{Na}^+$ ) and
3. Intermediates ( $\text{Al}^{3+}$ ,  $\text{Ti}^{4+}$ )

The network modifiers in the glass, such as  $\text{Na}^+$ ,  $\text{Ca}^{2+}$ ,  $\text{Ba}^{2+}$  and  $\text{Sr}^{2+}$ , create an excessive -ve charge by disrupting the Si-O-Si bonds, thereby, resulting in the formation of NBOs in the set cement. On the other hand, all the Bos found in the matrix were  $\text{O}_2$ . Therefore, by addition of other oxides such as CaO and  $\text{Na}_2\text{O}$  (network modifiers) in the glass composition NBOs can be formed.

Loewenstein hypothesized the centre of each tetrahedra, which is linked by an oxygen atom to another tetrahedra, can be engaged by  $\text{Al}^{3+}$ , while the centre of the next one is engaged by  $\text{Si}^{4+}$  or different ion carrying four or more positive charge (Loewenstein, 1954). Since  $\text{Al}^{3+}$  is an intermediate, it can act as both a network modifier and a network former (Zachariasen, 1932). The inclusion of  $\text{Al}^{3+}$ , as a

network former, in the tetrahedra forces a change in the glass behaviour and results in a surplus negative charge on the structure ( $\text{AlO}_4^-$ ). Therefore, the network now has a surplus negative charge, which must be balanced out by incorporating a network modifier to regain neutrality. The substitution of  $\text{Si}^{4+}$  by  $\text{Al}^{3+}$  ions in the glass can happen only to the point of ratio limit 1:1. This ratio is critical, and should be ideally 1.2:1 by mass if the glass is to be able to form a set cement (Wilson *et al.*, 1980).

Early work on the effect of  $\text{Al}_2\text{O}_3/\text{SiO}_2$  ratio in classic glass composition suggests that it was a crucial factor in determination of the glass reactivity. Fluxes containing  $\text{F}^-$  ( $\text{CaF}_2$  and  $\text{Na}_3\text{AlF}_6$ ) apart from lowering the glass fusion temperature, impart  $\text{F}^-$  release and recharge ability to the cement. (Kent *et al.*, 1979; Wilson *et al.*, 1980).

Based on the recommendations of ISO,  $\text{Ca}^{2+}$  is wholly or partially replaced by  $\text{Sr}^{2+}$  or  $\text{Ba}^{2+}$  or to make the set cement more radiopaque.  $\text{Sr}^{2+}$  is routinely employed for this purpose since it has an ionic radius similar to that of  $\text{Ca}^{2+}$  and hence can isomorphically replace it without disruption or producing any loss of translucency (Deb and Nicholson, 1999).

### **2.5.2 GIC Poly Acids**

The earliest experimental GIC (ASPA-I) system included a liquid component which was composed of a homopolymer of PAA 50% by mass and essentially had poor handling properties. This was found to be due to susceptibility to early gelation owing to intermolecular hydrogen bonds formation between the polymer chains (Crisp *et al.*, 1975b).

### 2.5.2 (a) Acrylic Acid and Itaconic or Maleic Acid Copolymers

It has been suggested that instead of only using homopolymers of PAA, copolymers of PAA with other carboxylic acids such as itaconic acid and maleic acid (Figure 2.3) can reduce polymer chain intermolecular hydrogen bonding owing to their reduced stereoregularity (McLean and Wilson, 1977).

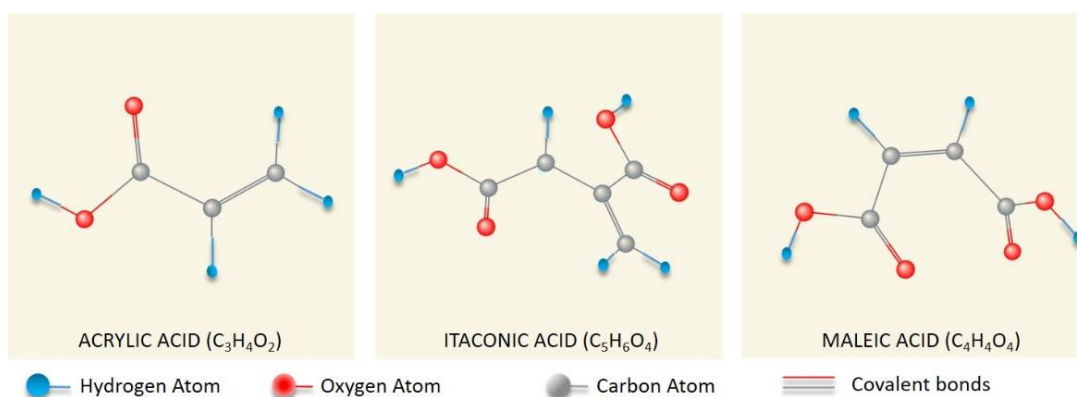


**Figure 2.3:** Illustration of the chemical structure of GIC polyacids

A reduced intermolecular hydrogen bonding was observed in these newer copolymers which was attributed to the presence of two COO groups resulting in higher degree of cross-linking in the copolymer. This newer PAA copolymer developed by Crisp *et al.*, containing an aqueous solution of acrylic acid, itaconic acid and tartaric acid was termed as ASPA-IV system (Crisp *et al.*, 1980). As a result, the first commercial GIC contained the PAA and itaconic acid copolymer formulation were developed (Crisp *et al.*, 1980). However, long term investigations on the influence of water storage on the biaxial flexure strength and compressive strength, of GICs based on copolymers of PAA demonstrated a decrease in biaxial flexural



strength on ageing compared with those based on homopolymers of PAA (Nicholson and Abiden, 1997; Williams and Billington, 1991). It has been suggested that the decrease in compressive strength of the copolymer containing GICs on long term water storage, may be a consequence of the high density of copolymers cross-linking rather than hydrolysis (Nicholson and Abiden, 1997; Pearson and Atkinson, 1991).

## **2.6 Setting Reaction of GICs**

The setting reaction of GICs is thought to be complicated and yet not fully comprehensible. Attempts have been made to observe and characterize this phenomenon using various qualitative and quantitative techniques, such as infrared, XRD, FTIR, and solid-state NMR spectroscopy (Crisp *et al.*, 1974; Pires *et al.*, 2004; Zainuddin *et al.*, 2009). When the glass powder and the PAA solution are spatulated into each other, a paste is produced, which signifies the beginning of an acid-base reaction. The GIC sets and hardens via metal ions transfer from the glass particles to matrix which results in gelation of the aqueous phase (Anusavice, 2003; Craig *et al.*, 2006; Wilson and Kent, 1971; Wilson and Kent, 1972; Wilson and McLean, 1988; Wilson and Nicholson, 1993; Wilson, 1991; Wilson and Crisp, 1975).

During the cascading transfer of these ions, the cement matrix is vulnerable to moisture because the liberated metal ions are in a soluble form. Desiccation of the cement is another cause of early solubility as it causes water loss which can disrupts the cement architecture. However, desiccation after cement maturation is no longer a concern. The acid and powder when mixed attacks the surface of the basic glass particles producing a paste like mixture. Several authors have verified the existence of

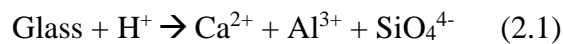
three phases during the setting of GICs (Kent *et al.*, 1979; McLean and Gasser, 1985; Mount, 2002; Smith, 1998; Wilson and Kent, 1971; Wilson and Kent, 1972; Wilson and McLean, 1988; Wilson and Nicholson, 1993; Zachariasen, 1932).

### 2.6.1 Ion-Leachable Phase

The first phase is best described as the ion extraction phase as the metal ions are released during this stage. The ionization of the carboxylic acid liberates H<sup>+</sup> protons from the carboxyl (COO) group. These H<sup>+</sup>, when they reach a saturation point, attack the surface of the glass particles releasing a cacophony of Al<sup>3+</sup>, Ca<sup>2+</sup>, Na<sup>+</sup>, F<sup>-</sup> in non-sequential manner (Figure 2.4), and H<sub>2</sub>PO<sub>4</sub><sup>-</sup> ions into the matrix (Wilson and Prosser, 1982).

In a study it was found that this acid attack was nonuniform and appeared to be concentrated at Ca<sup>+</sup> rich sites on the glass surface as these were the more basic sites (Barry *et al.*, 1979). Regardless of the location of the attack, it results in the production of silicic acid (SiO<sub>4</sub>) which later forms a silicious hydro gel (Si(OH)<sub>4</sub>•X(H<sub>2</sub>O)) around the unreacted glass crystals which then act as fillers (Wasson and Nicholson, 1990; Wilson and Nicholson, 1993).

The setting reactions can be represented by the following equations (Darvell, 2018):



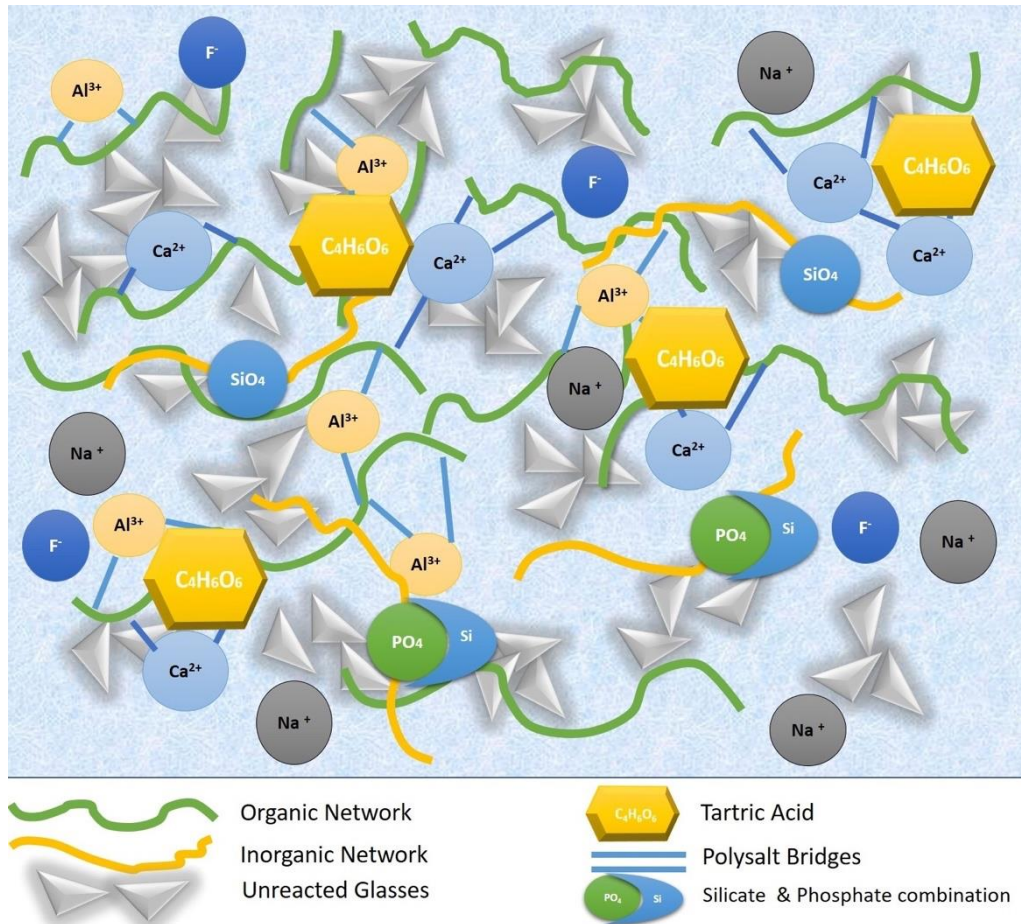


**Figure 2.4:** Schematic illustration of what is thought to occur during the setting reaction of GICs.

A couple of studies tried to determine the quantity of glass particles consumed in the acid attack. One group of researchers predicted that roughly in the range of 20-30% glass particles are consumed, while in another study, Billington *et al.*, (2007) countered that approximately 7% of the glass is degraded within the cement matrix. This degradation of the glass particles and cross-linking of the polyacids chains with poly salt bridges is accompanied with a rise in the viscosity and pH of the cement paste (Billington *et al.*, 2007; Crisp and Wilson, 1974)